Cold collisions of PH ($^3\Sigma^-$) with helium in magnetic fields

Eryin Feng,[*] Chunhua Yu, Chunyan Sun, Xi Shao, and Wuying Huang

Department of Physics, Anhui Normal University, Wuhu 241000, People's Republic of China
(Received 9 November 2011; published 13 December 2011)

A theoretical investigation of the He-PH ($^3\Sigma^-$) complex is presented. We perform *ab initio* calculations of the interaction potential energy surface and discuss its error bounds with relevance to cold collisions, and we carry out accurate calculations of bound energy levels of the complex including the molecular fine structure and magnetic-field effect. We find the potential has two shallow minima and supports ten and 13 bound levels in complex with ^{3}He and ^{4}He, respectively. Based on the potential the quantum scattering calculations are then implemented for elastic and inelastic cross sections of the magnetically trappable low-field-seeking state of PH ($^3\Sigma^-$) in collision with ^{3}He atom. The cold-collision properties and the influence of the external magnetic field as well as the effect of the uncertainty of interaction potential on the collisionally induced Zeeman relaxation are explored and discussed in detail. The ratio of elastic to inelastic cross sections is large over a wide range of collision energy, magnetic field, and scaling factor of the potential, so that helium buffer-gas loading and evaporative cooling of PH is a good prospect.

I. INTRODUCTION

Over the last decade, there has been continuous experimental progress in cooling and trapping molecules. At present, ultracold molecules can be produced by a wide variety of approaches, such as photoassociation of atoms at microkelvin temperatures [1–3], molecular beam deceleration [4,5], or buffer-gas loading followed by evaporative cooling in a magnetic trap [6,7]. Among these methods, the helium buffer-gas loading technique is applicable to any paramagnetic species and is the most universal method to cool down molecules. It employs a gas of ^{3}He atoms and involves the capture of molecules in a gradient magnetic trap for further evaporative cooling. Magnetic trapping selects molecules in the low-field-seeking states whose energy increases with increasing magnetic field. Whereas the low-field-seeking states are always instable, it may undergo inelastic relaxation in collisions with helium atoms at cold and ultracold temperatures, leading to trap loss. The efficiency of buffer-gas cooling depends critically on the ratio of elastic energy transfer and Zeeman relaxation in collisions with ^{3}He atoms.

It is expected that the interaction potential of helium atom and molecules in Σ—or atoms in *S*—electronic states should have less anisotropy and will be far more robust against helium-induced Zeeman relaxation than molecules or atoms in states with projection of electronic orbital angular moment $\Lambda \neq 0$. Investigation of the Zeeman relaxation of these types of species is of importance for buffer-gas cooling. Many experimental works have been devoted to this subject for molecules [8–14] and for atoms [15,16] in the past few years. The first successful buffer-gas cooling and magnetic trapping of molecules was accomplished with a CaH ($^2\Sigma$) molecule at a temperature of about 0.4 K [7]. Later, another $^2\Sigma$ molecule, CaF, was also buffer-gas cooled [10]. The technique was further successfully extended to molecules with high spin electronic ground state, including NH and ND $^3\Sigma$ molecules,

[11–13], VO $^4\Sigma$ molecules [8], and CrH $^6\Sigma$ and MnH $^7\Sigma$ molecules [14].

The experimental success in the buffer-gas cooling and trapping of molecules also stimulates theoretical investigations on the understanding of collisional energy transfer. Many of them are dedicated to Zeeman relaxation of diatomic molecules in a Σ state in collisions with ^{3}He at low temperature and submitted to a magnetic field. Volpi and Bohn [17,18] studied the He-O$_2$ collision and magnetic-field effects, and showed that the collisionally induced Zeeman relaxation in this system is slow. Krems and Dalgarno [19] developed the formal theory of collisions between atom and molecule in the presence of a magnetic field, and applied it to the He-CaH ($^2\Sigma$) [20,21] and He-NH ($^3\Sigma$) [22,23] collisions. They indicated the molecules with large rotational constants and small spin-rotation constants should be least efficient for Zeeman relaxation processes. For the He-NH ($^3\Sigma^-$) system, González-Martínez and Hutson [24] located two very narrow zero-energy Feshbach resonances. Very recently, Turpin *et al.* [25] studied the Zeeman relaxation of a high spin electronic state molecule, MnH ($^7\Sigma^+$), in collisions with ^{3}He and gave a comparison with experiment. Stoecklin and Gianturco and coworkers further extended the study to the ionic molecule collision: He-N$_2$$^+$ ($^2\Sigma$) [26–28], He-OH$^-$($X\,^1\Sigma^+$) [29], He-OH$^+$($^3\Sigma^-$) [30], and He-LiH$^-$($X\,^2\Sigma^+$) [31].

In the present work, we investigate the low-energy collisions of ground-state PH ($^3\Sigma^-$) molecule with He atoms in a magnetic field based on an *ab initio* interaction potential. The ground electronic state of PH molecule has the same $^3\Sigma^-$ symmetry as NH molecule. Helium buffer-gas loading and magnetic trapping experiments of the NH molecules have been successfully performed [11,13]. There are also extensive theoretical works on the cold collisions of the He-NH system [22–24]. Here, the main purpose of this work is to provide a proposal of whether or not the PH ($^3\Sigma^-$) is a good candidate to be cooled using buffer-gas cooling and stored using magnetic trapping through our theoretical calculation.

The paper is organized as follows. In Sec. II, the *ab initio* calculations of the interaction potential energy are briefly

_____
[*]fengbf@mail.ahnu.edu.cn

described and the uncertainty of the potential is discussed. In Sec. III, the method used for the calculating of bound states and the theoretical results are presented. In Sec. IV, we briefly recall the main steps of the close-coupling calculations, and give results and discussions in detail.

II. THE POTENTIAL ENERGY SURFACE AND ITS UNCERTAINTY

The He-PH system can be described by the usual Jacobi coordinates: R, the distance between the He atom and the center of mass of the PH molecule; r, the PH bond distance; and θ, the angle between R and r. $\theta = 0°$ corresponds to the He-P-H collinear configuration. The PH bond distance was frozen at its experimental equilibrium geometry ($2.687a_0$) [32]. Preliminary close-coupling with single and double excitation (CCSD) calculations of the He-PH system have shown that the T_1 diagnostic (~ 0.008) and the D_1 diagnostic (~ 0.017) both are smaller than the corresponding usual cutoff values of 0.02 and 0.025 [33], indicating that a single reference wave function is able to accurately describe the system. The partially spin-restricted open-shell single and double excitation coupled cluster method with perturbative triples [RCCSD(T)] method was thus used to determine the potential energy surface (PES) for the He-PH ($^3\Sigma^-$) complex. We employed the aug-ccpV5Z basis set of Woon and Dunning [34] for the three atoms, augmented by the $(3s3p2d2f1g)$ set of midbond functions with exponents of 0.90, 0.30, 0.10 for the s and p functions, 0.60, 0.20 for the d and f functions, and 0.30 for the g function. The bond functions were placed at mid-distance between the PH center of mass and He. The Boys and Bernardi [35] counterpoise procedure was used to correct for basis set superposition error. Calculations were done at a total of 210 geometries. The values of R ranged from $4.5a_0$ to $20a_0$ and the angular θ grid varied at every $30°$ spacing from $0°$ to $180°$. It is notable that the $X^3\Sigma^-$ state of PH is odd under reflection in the plane containing the PH axis, and for nonlinear He-PH geometries the electronic ground state of the complex has A'' symmetry under reflection in the plane containing all the nuclei. All the calculations were carried out using the MOLPRO 2006 package [36].

In order to facilitate the following applications, we adapted the two-step fitting procedure described in our previous papers [37–39] to obtain an analytic representation of the PES. Over the entire grid, the global rms error between the analytic fit and the *ab initio* points is 0.0159 cm^{-1} and the maximum absolute error is 0.0439 cm^{-1}. In the region of the potential well, the absolute error is less than 0.1 cm^{-1} and the relative error is less than 0.015%. In the long range, the relative error is within 0.7%. A FORTRAN subroutine for generating the two-dimensional PES is available upon request.

Figure 1 shows the contour plot of the PES of He-PH complex. It has two minima on the potential energy surface with comparable depths. The global minimum with energy of -17.10 cm^{-1} locates at $R = 7.65a_0$ and $\theta = 134.0°$, and the second minimum is -16.88 cm^{-1} at $R = 7.44a_0$ and $\theta = 0°$. The two minima are separated by a saddle point at $R = 7.86a_0$ and $\theta = 80.55°$ with a barrier height of 5.4 cm^{-1} relative to the global minimum. Compared with the He-NH system (Fig. 2 in
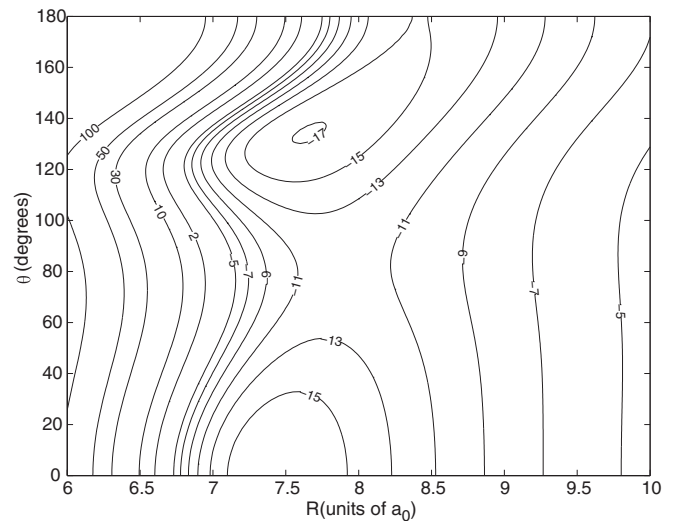

FIG. 1. Contour plot (units of cm^{-1}) of the He-PH potential energy surface.

Ref. [23]), the PES of the He-PH complex is more anisotropic, predicting larger inelastic cross sections in the collision of PH with He.

An important problem is that scattering calculations at very low energies depend strongly on the details of the interaction potential. We thus further make an estimation of error bounds for calculated interaction energies. The largest contributions to the uncertainty in the interaction potential arise from the approximate treatment of electronic correlation and the incompleteness of the electronic basis set. We expect that the effect of the neglecting vibrations of the PH molecule is much less important due to low collision energy.

For the first aspect, we performed eight-electron full configuration-interaction (FCI) calculations of the interaction energy with 6-31G basis set augmented with spd midbond functions (only a small basis set is possible used in FCI). We included all electrons arising from the H and He atoms and the $3s3p$ electrons of the P atom. The FCI correlation energy was found to be larger than the RCCSD(T) correlation energy by 0.15–0.25% for a wide range of R in the region of the potential well. To a good approximation we expect the ratio of these two correction energies to be constant in different basis sets. This suggests that the global minimum energy obtained with the coupled-cluster method is underestimated by ~ 0.04 cm^{-1}.

For the second aspect, we extrapolated the individual counterpoise-corrected interaction energy to the complete basis set (CBS) limit. The CBS limit value is obtained by three-point extrapolation [40] from values of the aug-cc-pVXZ ($X = $ T,Q,5) basis sets; at the global minimum this yields a depth of -17.29 cm^{-1}. This is 0.19 cm^{-1} more than in the method used for the complete surface here. We also performed test calculations including additional core-valence basis functions that are absent in the basis set used for the complete surface potential. The interaction energy at the global minimum obtained with aug-cc-pCV5Z is approximately 0.12 cm^{-1} smaller than for basis sets without core-valence functions.

In summary we can approximately set the error bounds on the interaction potential at the global minimum between –0.23 and +0.12 cm^{-1}, which is between -1.3% and $+0.7\%$.

III. BOUND-STATE CALCULATIONS

To obtain the rovibrational energy levels of the ^{3}He-PH and ^{4}He-PH molecules with the PES presented in Sec. II, we used the method analogous to that described in our previous papers [37–39]. Here we extend it to include the magnetic-field effect. The Hamiltonian of the He-PH ($^3\Sigma^-$) complex in Jacobi coordinates (R,θ) is

$$\hat{H} = -\frac{\hbar^2}{2\mu R}\frac{\partial^2}{\partial R^2}R + \frac{\hat{L}^2}{2\mu R^2} + \hat{H}_{\rm PH} + V(R,\theta), \qquad (1)$$

where μ is the reduced mass of the complex, $\hat{L}$ is the rotation angular momentum associated with the intermolecular coordinate R, and $V(R,\theta)$ is the He-PH interaction potential. $\hat{H}_{\rm PH}$ denotes the Hamiltonian for the PH ($^3\Sigma^-$) monomer and is expressed as:

$$\hat{H}_{\rm PH} = b_{\rm PH}\hat{N}^2 + \gamma\hat{N}\cdot\hat{S} + \frac{2}{3}\lambda_{SS}\sqrt{\frac{24\pi}{5}}$$
$$\times\sum_q (-1)^q Y_{2-q}(r)[\hat{S}\otimes\hat{S}]_q^2 + \hat{H}_z, \qquad (2)$$

where $b_{\rm PH} = 8.412518$ cm^{-1} is the rotational constant of PH in its ground vibrational level [32], and $\hat{N}$ and $\hat{S}$ are the rotational and spin angular momenta of the monomer molecule. The spin-rotation and spin-spin interaction constants are $\gamma = -0.076916$ cm^{-1} and $\lambda_{SS} = 2.20969$ cm^{-1} [32]. The Zeeman Hamiltonian H_z, neglecting rotational and anisotropic spin terms, is

$$H_Z = g_e\mu_B\hat{B}\cdot\hat{S}, \qquad (3)$$

where g_e is the g factor for the electron, μ_B is the Bohr magneton, and $\hat{B}$ is the magnetic-field vector.

In the presence of a magnetic field, total angular momentum J is not a good quantum number; the only rigorously good quantum numbers are the total parity which is given by $p = (-1)^{N+L+1}$ and the total angular momentum projection $M_J = M_N + M_S + M_L$, where M_N, M_L, and M_S are the projections of $\hat{N}$, $\hat{L}$, and $\hat{S}$ individually. There are several basis sets that could be used to expand the eigenfunctions of Eq. (1). We used an uncoupled basis set $|\chi_q(R)\rangle|NM_N\rangle|SM_S\rangle|LM_L\rangle$ [24]. States with $N\leqslant 6$ and $L\leqslant 8$ were included in the angular basis set $|NM_N\rangle|SM_S\rangle|LM_L\rangle$. The quantum numbers take all values allowed by conservation of M_J and parity p. The radial basis $|\chi_q(R)\rangle$ was determined as numerical eigensolutions to the vibrational Schrödinger equation [37–39],

$$\left[-\frac{\hbar^2}{2\mu}\frac{\partial^2}{\partial R^2} + V(R,134°)\right]\chi_q(R) = E_q\chi_q(R), \qquad (4)$$

where $V(R,134°)$ is a cut of the He-PH interaction potential at an angle of 134° corresponding to the global minimum of potential. The required angular matrix elements of operators in Eq. (1) can be found in Ref. [24] and radial matrix elements were calculated by numerical integration. The eigenvalues and eigenfunctions of the Hamiltonian are determined from solution of the corresponding secular equation.

TABLE I. Bound levels of He-PH complex. All the levels correspond to the approximate quantum numbers $N = 0$ and $j = 1$. Energies are relative to the ground-state energy of PH ($X\,^3\Sigma^-$) which is -0.088 cm^{-1}.

J	Parity	L	^{3}He-PH Energy (cm^{-1})	^{4}He-PH Energy (cm^{-1})
1	–	0	–3.6651	–4.5018
0	+	1	–3.1636	–4.0982
1	+	1	–3.1451	–4.0767
2	+	1	–3.1326	–4.0621
1	–	2	–2.1305	–3.2410
2	–	2	–2.1234	–3.2328
3	–	2	–2.1103	–3.2173
2	+	3	–0.6587	–1.9988
3	+	3	–0.6543	–1.9934
4	+	3	–0.6415	–1.9770
3	–	4		–0.4051
4	–	4		–0.4014
5	–	4		–0.3865

The bound-state levels of the ^{3}He-PH and ^{4}He-PH complexes with zero magnetic field are listed in Table I. The energies are relative to the ground-state energy of PH ($^3\Sigma^-$) which is -0.088 cm^{-1}. The binding energies, –3.6651 and –4.5018 cm^{-1}, of the two complexes are small compared with the rotational constant $b_{\rm PH} = 8.412518$ cm^{-1} which means all bound levels correspond to the ground rotational state of PH with $N = 0$, $j = s = 1$. In zero field, the total angular momentum J is conserved and $J = L, L\pm 1$. The ground level of the complex is associated with $L = 0$ and odd parity, while the excited levels of the ^{4}He-PH complex correspond to $L = 1$–4 and the ^{3}He-PH complex with $L = 4$ is unbound. The three different J excited levels corresponding to each value of L are not threefold degenerate as the spin-spin and spin-rotation interactions, but are close together: Separations are only about 0.01 cm^{-1}. As can be seen, there are ten bound levels in the complex with ^{3}He while 13 bound levels in the complex with ^{4}He. Though the well depth of He-PH is slightly shallower than that of He-NH, the number of bound levels in He-PH is three more than in He-NH complex [23] due to larger reduced mass of He-PH complex.

In the presence of a magnetic field, J is no longer conserved. The energy is characterized by the M_J and parity p. L remains an essentially good quantum number except in the vicinity of the avoided crossings. Figure 2 shows the bound-state energies of ^{3}He-PH for $M_J = 0$ and $M_J = -1$ as a function of magnetic field. Each level splits into components that can be labeled with the approximate quantum numbers $Mn = 0$ and $Ms = 0, \pm 1$. For different $M_J \neq 0$, some Ms levels are missing and there are also small shifts of the energy levels with the same L value. As expected, the Zeeman splits are approximately linear for He-PH in the range of fields studied. This is because for $N = 0$ state the coupling arises from the off-diagonal term of $V(R,\theta)$ and the spin-spin interaction that mixes the excited N levels, but the spacing (~ 16.8 cm^{-1}) between $N = 0$ and $N = 1$ levels for PH is larger than the Zeeman split tuned by the magnetic field. There is an avoided crossing at about 1.2 T
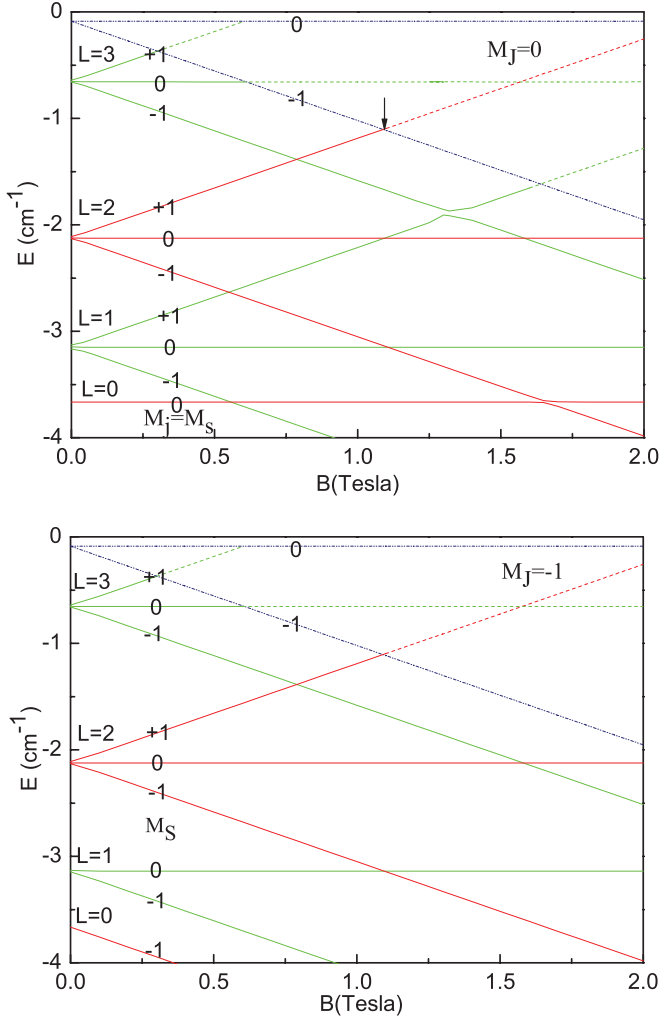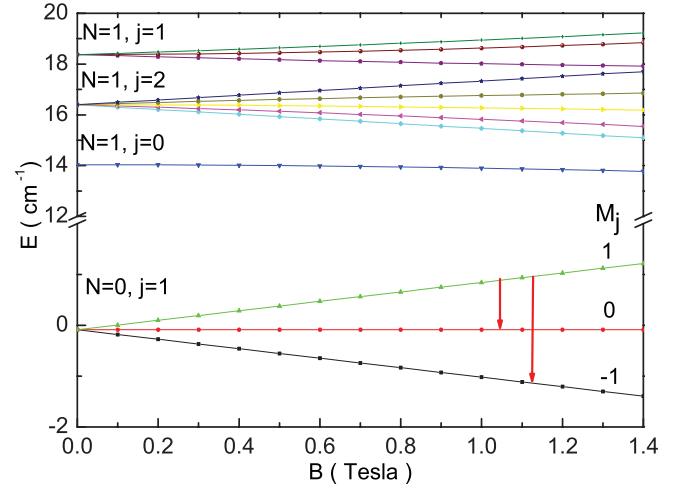
FIG. 3. (Color online) Diatomic eigenenergies of the PH ($^3\Sigma^-$) monomer Hamiltonian as a function of the applied magnetic field. The value of M_j is reported on each curve of the $N = 0$. The Zeeman relaxation transitions originating from the $N = 0$, $M_j = 1$ level are also represented.

FIG. 2. (Color online) Bound-state energy levels of ^{3}He-PH for $M_J = 0$ (upper panel) and $M_J = -1$ (lower panel) as a function of magnetic field.

field for $M_J = 0$ where levels of the same M_J and parity but different M_S cross.

IV. SCATTERING CALCULATIONS AND RESULTS

A. Method

The method developed by Krems and Dalgarno [19] and González-Martínez and Hutson [24] was employed to treat collisions between He atom and PH ($^3\Sigma^-$) molecule in the presence of a magnetic field. The Hamiltonian of the He-PH collision system in a magnetic field has been given in Eq. (1). For the bound-state calculation, an uncoupled angular basis set $\phi_i = |N M_N\rangle |S M_S\rangle |L M_L\rangle$ was used. The asymptotical Hamiltonian in Eq. (2) is not diagonal in the uncoupled basis set ϕ_i which then cannot be used to describe the asymptotic states of the dressed molecule in the presence of the field. We use instead a transformation basis set $\chi_\alpha = \Sigma_i C_{\alpha i} |N M_N\rangle |S M_S\rangle$ [26], which diagonalizes the monomer Hamiltonian (2),

$$[C H_{PH} C^{-1}]_{\alpha\beta} = \xi_\alpha \delta_{\alpha\beta},$$ (5)

where ξ_α is the energy level of the dressed diatomic molecule in the magnetic field represented in Fig. 3. The magnetic field removes the degeneracy in $M_j = M_N + M_S$ and each energy level ξ_α correlating with a unique value of M_j labeled by $M_j(\alpha)$, where j is the total angular momentum of the diatomic molecule, $\hat{j} = \hat{N} + \hat{S}$, and Mj is its projection. For a given value of M_J and for a given M_j, the $M_L = M_j(\alpha) - M_j(\alpha)$. The basis set describing the collision process is obtained by including the possible values of the quantum number L for each value of α. With the basis set, the close-coupling equation is

$$\left\{ \frac{d^2}{dR^2} - \frac{L(L+1)}{R^2} + 2\mu[E - \xi_\alpha] \right\} F_{\alpha,M_L,L}(R)$$

$$= 2\mu \sum_{\alpha',M_L',L'} [C^T U C]_{\alpha,M_L,L}^{\alpha',M_L',L'} F_{\alpha',M_L',L'}(R).$$ (6)

The cross sections for elastic and inelastic scattering were computed from the S matrix as follows:

$$\sigma_{\alpha \to \alpha'} = \frac{\pi}{k_\alpha^2} \sum_{M_J} \sum_{M_L L} \sum_{M_L' L'} \left| \delta_{\alpha\alpha'} \delta_{M_L M_L'} \delta_{LL'} - S_{\alpha L M_L; \alpha' L' M_L'}^{M_J} \right|^2.$$ (7)

The coupled equations were propagated on a radial grid ranging from $6a_0$ to $200a_0$ in steps of $0.25a_0$ using the log-derivative propagator of Johnson [41]. At ultralow collision energies, s-wave scattering dominates the collision dynamics and calculations can be performed with a small number of partial waves. We carried out convergence tests on state-to-state cross sections both in the s-wave regime and at energies up to $E = 10$ cm^{-1}, at fields up to 2 T. In all cases a basis set with $N = 0 \ldots 5$ and $L = 0 \ldots 8$ gave convergence to within approximately 5% for all state-to-state cross sections. This basis set was therefore used in all the remaining calculations.

B. Results and discussions

As shown in Fig. 3, the low-field-seeking state which can be magnetically trapped is the state with $N = 0$, $M_j = 1$ of PH ($^3\Sigma^-$). It can relax to lower-energy states with $N = 0$, $M_j = 0$, -1 through inelastic collisions. Figure 4 shows the elastic and M_j changing cross sections for this trappable state in the absence of magnetic field which corresponds approximately to the situation of the center of a trap [42]. We can see that the cross section for the M_j changing Zeeman relaxation is much smaller than the elastic cross section and decreases as E^2 with decreasing collision energy below $\sim 10^{-1}$ cm^{-1}. It can be understood by Wigner's threshold law for isoenergetic processes [43,44]:

$$\sigma \propto E^{L+L'}, \qquad (8)$$

where L and L' denote the partial waves in the incoming and outgoing channels, respectively. At low collision energies, the cross sections are dominated by incoming s waves. For elastic collisions, we have $L = L' = 0$ and the cross section is constant as a function of collision energy E. For inelastic collisions, the change in M_j must be accompanied by a change of the M_L quantum number, which follows from the conservation of M_J. Since the parity p is also conserved, it is easily found that the dominant inelastic process for the incoming s wave of PH corresponds to the $L' = 2$ outgoing channel, and consequently exhibits E^2 behavior as observed in Fig. 4. The presence of a d wave centrifugal barrier in the exit channel, whose height is about 0.3 cm^{-1} for ^{3}He-PH, strongly suppresses the inelastic transitions for low collision energies.

The cross sections also show two main resonant structures. The elastic cross section varies by about one order of magnitude through the resonance, while the spin-flipping cross section increases by three to four orders of magnitude for the large peak. The cross sections do not show any resonance enhancement with only $L = 0 \ldots 3$ channels, whereas adding the $L = 4$ channels produces the large peak at the collision energy of about 1.6 cm^{-1}; adding further the $L = 5$ channels produces the small peak at about 3 cm^{-1}. Thus both the peaks

FIG. 5. (Color online) The Zeeman relaxation cross sections of PH ($N = 0$, $M_j = 1$) in collisions with ^{3}He as a function of collision energy with an applied magnetic field.

in Fig. 4 arise from shape resonances and the $L = 4$ shape resonance is responsible for the large peak and the $L = 5$ shape resonance for the small peak. Shape resonance is due to coupling of the scattering state with a quasibound level trapped behind a repulsive barrier. We note that the barrier height of $L = 4, 5$ is about 2.2 and 4.3 cm^{-1} for ^{3}He-PH, respectively.

Investigation of the behavior of the molecules in a magnetic field is essential to understanding magnetic trapping. The cross sections as a function of collision energy with different magnetic-field strengths are given in Fig. 5. The inelastic cross sections are summed over both the $M'_j = 0$ and $M'_j = -1$ Zeeman relaxation channels. The elastic cross sections are weak dependence with the magnetic field which is thus not reported in the figure for the sake of clarity. The first feature is that the relaxation cross sections increase to infinity in agreement with the Wigner law while the collision energy vanishes. When the field increases, the low-energy cross sections are substantially pushed up, but at higher energies the cross sections are less sensitive to the field. The mechanism has been explained by Tiesinga *et al.* [45] and Volpi and Bohn [18], which is based on the removal of the degeneracy of the initial and final channels when the field is applied. In a finite magnetic field, the Zeeman transitions are determined by the centrifugal barrier in the outgoing channel. When the energy defect between the initial and final scattering states is small, the height of the centrifugal barrier in the final state can be larger than the initial energy of the system and the inelastic collision is suppressed by the centrifugal maximum in the outgoing channel. As the magnetic field increases, the energy gap between the initial and final states becomes greater than the centrifugal barrier, which may lead to escape over the barrier. Suppression of inelastic collisions thus decreases and the Wigner upturn point moves to higher energy with increasing magnetic field. Eventually, the inelastic cross section reaches a maximum at a field of about 1 T and starts to decrease again. Another interesting feature of this figure is the monotonous lowering of the two resonance peaks when the strength of the field is increased while its position and width are conserved. It can be understood as a simple consequence of the increase of
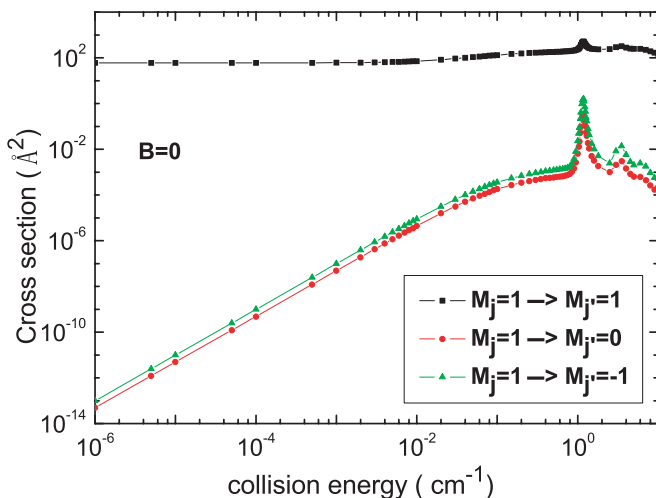

FIG. 4. (Color online) The cross sections for spin-flipping and elastic scattering transitions of PH ($N = 0$, $M_j = 1$) in collisions with ^{3}He in the absence of magnetic field.
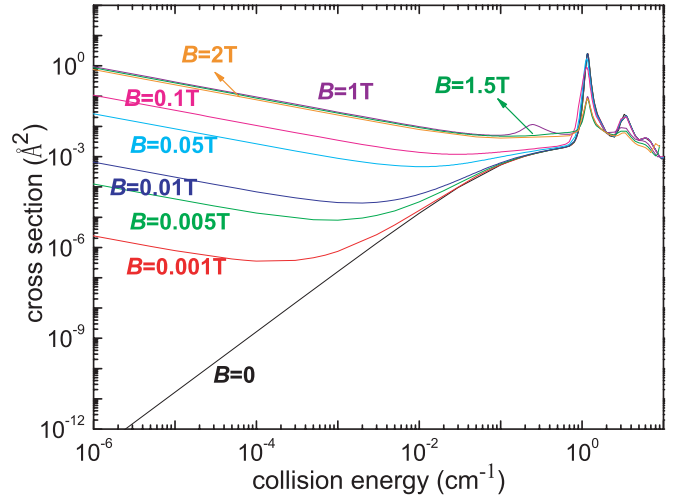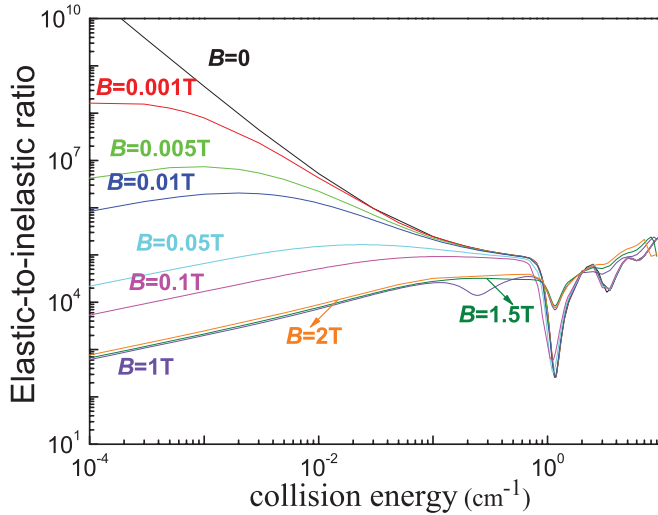
FIG. 6. (Color online) Ratio of the cross sections for elastic scattering and Zeeman relaxation in collisions of PH ($N = 0$, $M_j = 1$) with ^{3}He atoms with different applied magnetic field.
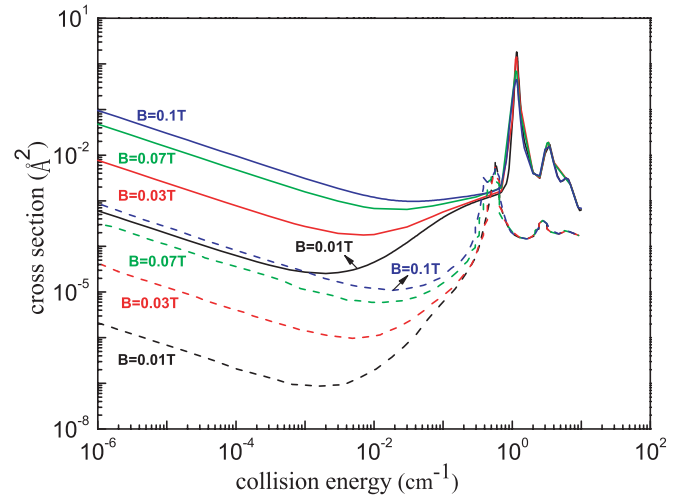

FIG. 7. (Color online) Comparison of the cross sections for Zeeman relaxation in ^{3}He-PH (in solid curve) and ^{3}He-NH collisions (in dashed curve).

the splitting between the $N = 0$, $j = 1$, and $M_j = -1$ and the excited levels ($N = 2$, $j = 1, 2$ and $M_j = 1$) with increasing field [19], resulting from the decrease of the coupling between coupled Zeeman levels. This effect is amplified for $B = 2$ T as the peak is more than two orders of magnitude smaller than in the absence of a field.

In order to make definitive predictions as to the efficiency of the buffer-gas loading, an analysis of the elastic-to-inelastic ratio as a function of collision energy and magnetic field over a wide range is needed. Figure 6 presents the ratios of cross sections for elastic scattering and Zeeman relaxation in ^{3}He-PH collisions in several values of magnetic fields and collision energies from 10^{-4} to 10 cm^{-1}. We find that the ratio is always more than 100 over the whole range of magnetic fields and kinetic energies considered here, suggesting that evaporative cooling of PH in a magnetic trap is likely to be efficient. It can also be seen that, in the ultracold regime, the ratio increases dramatically if the magnetic-field strength is reduced. Thus, once the cooling process has started in the subkelvin regime at relatively high magnetic field and continues toward lower energies as the magnetic trap depth is decreased, the ratio will remain very favorable for evaporative cooling to take place. We also calculated the thermally averaged rate constants. The elastic scattering rate constant is independent of the magnetic field. It has a magnitude of the order of 10^{-10} cm^3 s^{-1} at temperatures 0.5–1 K. The corresponding Zeeman rate constants in this temperature range decrease from the order of 10^{-13} to 10^{-15} cm^3 s^{-1} as fields from 0 to 2 T.

It is instructive to compare the cross sections for Zeeman relaxation in ^{3}He-PH and ^{3}He-NH collisions. Krems and Dalgarno [19] demonstrated that collision-induced spin depolarization in $^3\Sigma^-$ molecules is mediated by a small admixture of the anisotropic rotational state $N = 2$ in the rotational ground state ($N = 0$) of the molecule due to the spin-spin interaction. The collision-induced Zeeman relaxation cross section is then predicted to scale as λ_{ss}^2/B_e^2. This propensity rule has been demonstrated by a subsequent experiment [13]. The ratio of λ_{ss}^2/B_e^2 for PH is about 20 times more than for NH.

Figure 7 compares the cross sections for Zeeman relaxation in ^{3}He-PH and ^{3}He-NH collisions. The cross section for Zeeman transitions in PH is more than two orders of magnitude larger. The fact that the actual ratio is much larger (10^2–10^3) is due to the different anisotropies of the He-PH and He-NH interaction potentials. The equilibrium distance of PH is $2.687a_0$ and that of NH is $1.96a_0$. The PH molecule is more stretched than NH and the interaction potential of the He-PH complex is more anisotropic than the He-NH potential.

Zero-energy Feshbach resonances (ZEF) are currently used to produce condensates of diatomic molecules from an ultracold gas of atoms [46]. Such resonances also appear in collisions between atoms and molecules in the presence of an applied magnetic field and could be potentially used to produce ultracold complexes [24,47]. An s-wave scattering ZEF occurs at which the bound-state energies cross a threshold if a $L = 0$ scattering channel is permitted by the constraints on parity and M_J. This occurs only for thresholds corresponding to $M_j = M_J$ as shown by the arrow in Fig. 2. It can be seen
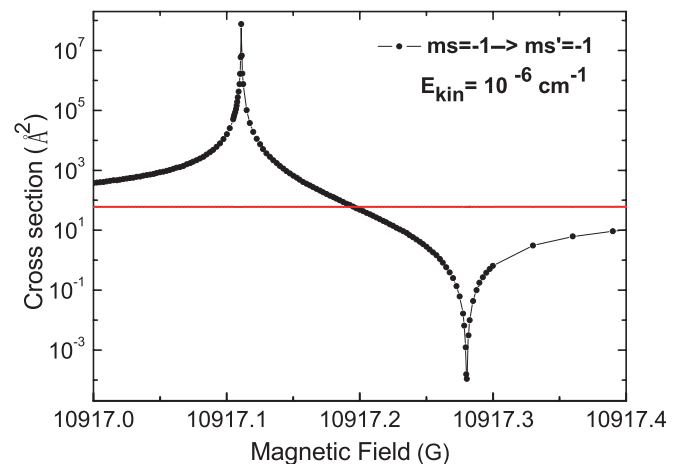

FIG. 8. (Color online) Elastic $M_S = -1 \rightarrow M'_S = -1$ transitions for ^{3}He-PH collisions in the vicinity of an elastic Feshbach resonance calculated at a kinetic energy of 10^{-6} cm^{-1}.
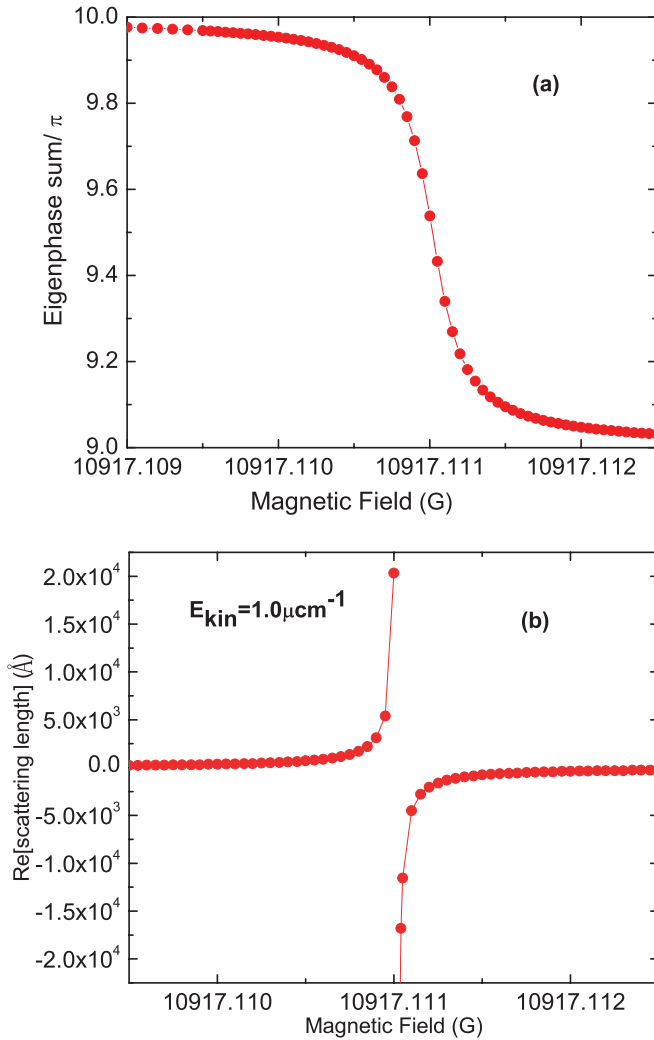
FIG. 9. (Color online) Eigenphase sum (a) and scattering length (b) for elastic $M_S = -1 \rightarrow M_S' = -1$ transitions for ^{3}He-PH collisions in the vicinity of an elastic Feshbach resonance calculated at a kinetic energy of 10^{-6} cm^{-1}.

that there is a ^{3}He-PH bound state with $M_S = +1$ that crosses the $M_S = -1$ threshold at about 10 900 G. A detailed scan across a small range of fields in the vicinity and careful extrapolation of the bound-state energies with magnetic field give a more precise estimate of 10 917 G. Figure 8 shows the cross section as a function of field in the vicinity of the Feshbach resonance at a kinetic energy of 10^{-6} cm^{-1}. The corresponding eigenphase sum and scattering length are shown in Fig. 9. For ^{3}He colliding with PH ($M_j = -1$) at ultralow kinetic energy, only elastic scattering can occur. For $M_J = 0$ and parity $p = -1$, the basis set gives five open channels with $L = 0, 2, \dots, 8$. Scattering into the $L > 0$ channels is strongly suppressed by the centrifugal barriers. The cross section shows a very large peak and the scattering length passes through a pole at resonance. The line shape is analogous to Fano line shapes [48] in bound-free absorption spectra due to the interference between the bound and continuum. The bound-state contribution rises from zero to a peak at resonance while the continuum contribution drops from its background value to zero and changes sign at resonance.

When there is only a single continuum channel, there is a point near resonance where the bound and continuum contributions cancel completely. It is the situation observed here. Fitting the scattering length to the formula commonly used in atomic scattering,

$$a(B) = a_{bg}\left(1 - \frac{\Delta B}{B_0 - B}\right),\qquad(9)$$

gives position $B_0 = 10\,917.111$ G, width $\Delta B = 2 \times 10^{-4}$ G and background scattering length $a_{bg} = 8.6$ Å. For ^{4}He colliding with PH ($M_j = -1$), there is also a similar ZEF occurring at $B = 16\,865.908$ G.

As a final part of our discussion, we consider the sensitivity of the elastic-to-inelastic ratio to the interaction potential. We estimate the bounds on the accuracy of our potential to be between -1.3% and $+0.7\%$ of the well depth. We therefore performed test calculations using our interaction potential multiplied by a factor F ranging from 0.95 to 1.05. The value of the magnetic field represented is 0.01 T. The result is shown in Fig. 10. The general pattern remains essentially the same; only the low collision energy and the resonance regions are more strongly modified, while the energy region above the resonance is almost unchanged. The ratio values are found to be a monotonous function of the multiplying factor F. As can be seen, however, the calculated ratios exceed 100 for almost all values of F and all energies considered. This demonstrates that evaporative cooling of PH is feasible. Although we cannot predict which value of F corresponds most closely to the exact potential, we do expect that the sampled range of F is indicative of the range within which the exact potential lies, and hence we conclude that the probability for successful evaporative cooling is relatively large.
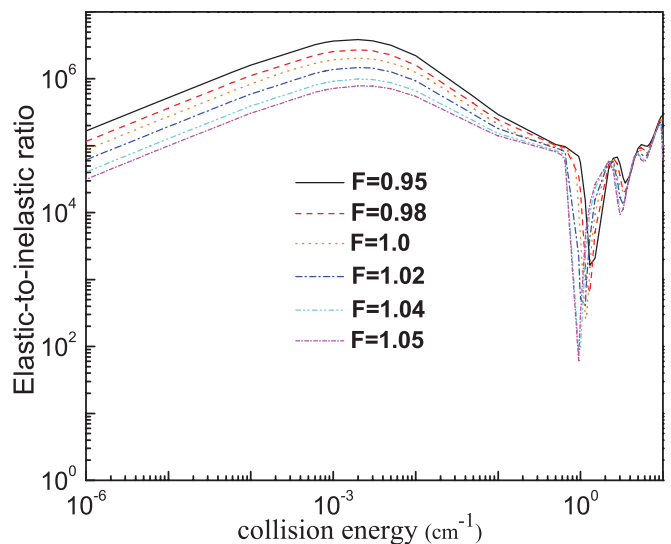

FIG. 10. (Color online) Ratio of the elastic-to-inelastic cross sections of PH ($N = 0$, $M_j = 1$) in collisions with ^{3}He as a function of collision energy using our model PES multiplied by a factor F ranging from 0.95 to 1.05. The value of the magnetic field represented is 10^{-2} T.

V. CONCLUSION

We have completed a comprehensive study of the He-PH complex. We have generated an accurate potential for the He-PH interaction based on supermolecular *ab initio* calculations incorporating the RCCSD(T) method, quintuple ζ basis set, and the basis set superposition error correction. The PES is weakly anisotropic and has two shallow minima with comparable depths. The global minimum with energy of -17.10 cm^{-1} locates at $R = 7.65a_0$ and $\theta = 134.0°$, and the second minimum is -16.88 cm^{-1} at $R = 7.44a_0$ and He-P-H collinear configuration. The bound energy levels of the complex have been calculated including the molecular fine structure. There are ten bound levels in the complex with ^{3}He while there are 13 bound levels in the complex with ^{4}He. The corresponding binding energies of the ^{4}He-PH and ^{3}He-PH complexes are found to be -4.50 and -3.67 cm^{-1}, respectively. Future spectroscopic measurement of these energies will provide a sensitive test of the potential surface. Bound-state energy levels of ^{3}He-PH as a function of magnetic field have also been investigated and then were used to locate a narrow zero-energy Feshbach resonance.

Based on the *ab initio* PES, we have used quantum mechanical scattering calculations to investigate the projection-change transitions in collisions of PH ($X\,^3\Sigma^-$) with He atoms within external magnetic fields at low and ultralow energies. We focused on the calculation of elastic and inelastic cross sections from low-field-seeking states with $N = 0$, $M_j = 1$ of PH ($^3\Sigma^-$) at different magnetic fields and kinetic energies. We found that the elastic cross section is weakly dependent with the magnetic field while the Zeeman relaxation cross sections rapidly increase with the magnetic-field strength at ultralow collision energies. Since collision-induced spin depolarization in $^3\Sigma^-$ molecules is mediated by a small admixture of the anisotropic rotational state $N = 2$ in the rotational ground state ($N = 0$) of the molecule, and the anisotropy is smaller than the separation between the $N = 0$ and 2 states, it causes relatively weak mixing during collisions and the scattering is generally elastically dominated. The inelastic cross sections are suppressed both at low energy and low field by the centrifugal barrier in the exit channels. However, the ratio of elastic to inelastic cross sections is high enough, over a wide enough range of collision energy, magnetic field, and scaling factor F of PES, indicating that helium buffer-gas loading and evaporative cooling of PH is a good prospect.

[1] A. Vardi, D. Abrashkevich, E. Frishman, and M. Shapiro, J. Chem. Phys. **107**, 6166 (1997).

[2] Y. B. Band and P. S. Julienne, Phys. Rev. A **51**, R4317 (1995).

[3] A. N. Nikolov, E. E. Eyler, X. T. Wang, J. Li, H. Wang, W. C. Stwalley, and P. L. Gould, Phys. Rev. Lett. **82**, 703 (1999).

[4] H. L. Bethlem, G. Berden, and G. Meijer, Phys. Rev. Lett. **83**, 1558 (1999).

[5] H. L. Bethlem, G. Berden, A. J. A. van Roij, F. M. H. Crompvoets, and G. Meijer, Phys. Rev. Lett. **84**, 5744 (2000).

[6] J. M. Doyle, B. Friedrich, J. Kim, and D. Patterson, Phys. Rev. A **52**, R2515 (1995).

[7] J. D. Weinstein, R. de Carvalho, T. Guillet, B. Friedrich, and J. M. Doyle, Nature (London) **395**, 148 (1998).

[8] J. D. Weinstein, R. de Carvalho, K. Amar, A. Boca, B. C. Odom, B. Friedrich, and J. M. Doyle, J. Chem. Phys. **109**, 2656 (1998).

[9] D. Egorov, J. D. Weinstein, D. Patterson, B. Friedrich, and J. M. Doyle, Phys. Rev. A **63**, 030501(R) (2001).

[10] K. Maussang, D. Egorov, J. S. Helton, S. V. Nguyen, and J. M. Doyle, Phys. Rev. Lett. **94**, 123002 (2005).

[11] W. C. Campbell, E. Tsikata, Hsin-I. Lu, L. D. van Buuren, and J. M. Doyle, Phys. Rev. Lett. **98**, 213001 (2007).

[12] E. Tsikata, W. C. Campbell, M. T. Hummon, H. I. Lu, and J. M. Doyle, New J. Phys. **12**, 065028 (2010).

[13] W. C. Campbell, T. V. Tscherbul, Hsin-I. Lu, E. Tsikata, R. V. Krems, and J. M. Doyle, Phys. Rev. Lett. **102**, 013003 (2009).

[14] M. Stoll, J. M. Bakker, T. C. Steimle, G. Meijer, and A. Peters, Phys. Rev. A **78**, 032707 (2008).

[15] C. I. Hancox, S. C. Doret, M. T. Hummon, L. J. Luo, and J. M. Doyle, Nature **431**, 281 (2004).

[16] T. V. Tscherbul, P. Zhang, H. R. Sadeghpour, A. Dalgarno, N. Brahms, Y. S. Au, and J. M. Doyle, Phys. Rev. A **78**, 060703(R) (2008).

[17] J. L. Bohn, Phys. Rev. A **62**, 032701 (2000).

[18] A. Volpi and J. L. Bohn, Phys. Rev. A **65**, 052712 (2002).

[19] R. V. Krems and A. Dalgarno, J. Chem. Phys. **120**, 2296 (2004).

[20] N. Balakrishnan, G. C. Groenenboom, R. V. Krems, and A. Dalgarno, J. Chem. Phys. **118**, 7386 (2003).

[21] R. V. Krems, A. Dalgarno, N. Balakrishnan, and G. C. Groenenboom, Phys. Rev. A **67**, 060703 (2003).

[22] R. V. Krems, H. R. Sadeghpour, A. Dalgarno, D. Zgid, J. Kłos, and G. Chałasiński, Phys. Rev. A **68**, 051401(R) (2003).

[23] H. Cybulski, R. V. Krems, H. R. Sadeghpour, A. Dalgarno, J. Kłos, G. C. Groenenboom, A. van der Avoird, D. Zgid, and G. Chałasiński, J. Chem. Phys. **122**, 094307 (2005).

[24] M. L. González-Martínez and J. M. Hutson, Phys. Rev. A **75**, 022702 (2007).

[25] F. Turpin, T. Stoecklin, and Ph. Halvick, Phys. Rev. A **83**, 032717 (2011).

[26] G. Guillon, T. Stoecklin, and A. Voronin, Phys. Rev. A **77**, 042718 (2008).

[27] G. Guillon, T. Stoecklin, and A. Voronin, Phys. Rev. A **75**, 052722 (2007).

[28] G. Guillon, T. Stoecklin, and A. Voronin, Eur. Phys. J. D **46**, 83 (2008).

[29] L. González-Sánchez, F. Marinetti, E. Bodo, and F. A. Gianturco, J. Phys. B **39**, 1203 (2006).

[30] L. González-Sánchez, E. Bodo, and F. A. Gianturco, Eur. Phys. J. D **44**, 65 (2007).

[31] D. López-Durán, M. Tacconi, F. A. Gianturco, Eur. Phys. J. D **55**, 601 (2009).

[32] R. S. Ram and P. F. Bernath, J. Mol. Spectrosc. **176**, 329 (1996).

[33] M. L. Leininger, I. M. B. Nielsen, T. D. Crawford, and C. L. Janssen, Chem. Phys. Lett. **328**, 431 (2000).

[34] D. E. Woon and T. H. Dunning, J. Chem. Phys. **100**, 2975 (1994).

[35] S. F. Boys and F. Bernardi, Mol. Phys. **19**, 553 (1970).

[36] MOLPRO, a package of *ab initio* programs designed by H.-J. Werner and P. J. Knowles; version 2006.1, R. Lindh *et al.*

[37] E. Y. Feng, Z. Q. Wang, M. Y. Gong, and Z. F. Cui, J. Chem. Phys. **127**, 174301 (2007).

[38] Z. Q. Wang, M. Y. Gong, Y. Zhang, E. Y. Feng, and Z. F. Cui, J. Chem. Phys. **128**, 044309 (2008).

[39] E. Y. Feng, C. Y. Sun, C. H. Yu, X. Shao, and W. Y. Huang, J. Chem. Phys. **135**, 124301 (2011).

[40] K. A. Peterson, D. E. Woon, and T. H. Dunning, J. Chem. Phys. **100**, 7410 (1994).

[41] B. J. Johnson, J. Comput. Phys. **13**, 445 (1973).

[42] J. D. Weinstein, R. de Carvalho, T. Guillet, B. Friedrich, and J. M. Doyle, Nature (London) **395**, 148 (1998).

[43] E. P. Wigner, Phys. Rev. **73**, 1002 (1948).

[44] R. V. Krems and A. Dalgarno, Phys. Rev. A **67**, 050704 (2003).

[45] E. Tiesinga, B. J. Verhaar, and H. T. C. Stoof, Phys. Rev. A **47**, 4114 (1993).

[46] S. Jochim, M. Bartenstein, A. Altmeyer, G. Hendl, S. Riedl, C. Chin, J. Hecker Denschlag, and R. Grimm, Science **302**, 2101 (2003).

[47] J. M. Hutson, M. Beyene, and M. L. Gonzalez-Martinez, Phys. Rev. Lett. **103**, 163201 (2009).

[48] U. Fano, Phys. Rev. **124**, 1866 (1961).